Soft Matter

Cite this: *Soft Matter*, 2012, **8**, 1096

www.rsc.org/softmatter

PAPER

Synthesis and thermal studies of aliphatic polyurethane dendrimers: a geometric approach to the Flory–Fox equation for dendrimer glass transition temperature†

Alison Stoddart,[a] W. James Feast[a] and Steve P. Rannard*[b]

Received 12th September 2011, Accepted 7th November 2011
DOI: 10.1039/c1sm06725g

A new convergent synthesis for polyurethane dendrons to generation 4, and dendrimers to generation 3, is presented with control of surface functionality. The systematic synthesis of twenty-six new dendritic materials has led to a study of the factors affecting T_g using widely accepted approaches. The established understanding of dendritic polymer T_g behaviour is that the Flory–Fox models, used for linear polymers, are unsuitable as the high number of chain ends and globular nature of dendrimers requires special consideration. In our review of the accepted understanding we have shown that the conventional Flory–Fox models predict $T_{g\infty}$ accurately and generate identical values to the established modifications of the Flory–Fox equation that consider 'dendrimer-relevant' aspects such as the non-zero values of n_e/M at infinite molecular weight. We also present a new approach using the geometric parameters of dendrimer mass evolution suggesting that the Flory–Fox equation is indeed appropriate for determination of dendrimer $T_{g\infty}$.

Introduction

Dendritic polymers[1] offer different properties to conventional linear polymers including encapsulation without prior self-assembly, shape persistence, tunable behaviour *via* multiple end group modification and, in the case of dendrimers, truly monodisperse molecular weight distributions.[2] The range of ideal dendrimer chemistries, synthesised by convergent or divergent growth strategies,[3] continues to grow and include polyesters,[4a] polycarbonates,[4b] polyamidoamines,[4c] polyamides,[4d,4e] polyamines,[4f] glycopeptides,[4g] polyethers,[4h] carbosilanes,[4i] phosphorous-containing materials,[4j] triazines[4k] and organometallic[4l] structures. The potential applications for dendrimers currently under investigation also continues to increase with catalysts,[5a] drug delivery/targeting,[5b] sensors,[5c] optical probes,[5a] solar cells and light harvesting,[5d] contrast agents,[5e] gene delivery[5f] and antimicrobials[5g] being among the most active areas. Polyurethanes remain a particular class of dendrimer chemistry that appears to be under-investigated. The effects of systematic structural differences on glass transition temperature (T_g) within this class of materials are also therefore not well reported.

Polyurethane dendrimers[6a,b] offer specific challenges during synthesis as conventional functionality used to generate carbamates (isocyanates and alcohols) are difficult to stabilise during the numerous reaction and purification steps required. A number of approaches using protected functionality, *e.g.* masked isocyanates, have been reported that lead to predominantly aromatic polyurethanes or dendrimers with mixed linking functionality eg urea-urethanes.[6c] We have reported previously hyperbranched polyurethane synthesis[6d] and a convergent route to aliphatic polyurethane dendrimers which benefited from the selective reactions of 1,1′-carbonyl diimidazole derivatives and produced dendrimers up to the third generation with N-*tert*-butoxycarbonyl surface functionality.[6a]

The T_g of dendrimers has been studied experimentally and using various modelling strategies. A recent report by Karatasos[7] utilised molecular dynamics simulations of varying generations of ideal dendrimer based on generalised AB_2 repeat units. Local intramolecular packing contributed significantly to the modelled thermal behaviour with intermolecular factors, through interpenetration, appearing to have a lesser contribution, especially with increasing generation. The study did not evaluate the effect of different topological features, *e.g.* surface groups and spacer length, or compare dendrons and dendrimers. Recent reviews[8a] and articles[8b,8c] have reiterated that dendrimer T_g is affected by end group substitution and correlated to a factor n_e/M, which

[a]*Interdisciplinary Research Centre in Polymer Science and Technology, University of Durham, Durham, DH13LE, UK*
[b]*Department of Chemistry, University of Liverpool, Crown Street, Liverpool, L69 7ZD, U.K. E-mail: srannard@liv.ac.uk; Fax: +44 151 794 3588; Tel: +44 151 3501*

† Electronic Supplementary Information (ESI) available: Synthesis details and structures for dendrimer and dendrons to generation 4; comparative analysis of T_g using conventional Flory–Fox, modified Flory–Fox and geometric progression equations for polyurethane dendrons and dendrimers; example data for $(n_e/M)_\infty$ determination; detailed analysis of dendrons and dendrimers from ref. 9 using conventional Flory–Fox, modified Flory–Fox and geometric progression equations and demonstrating approaches to calculate factors A, B and C. See DOI: 10.1039/c1sm06725g/

was first introduced by Wooley *et al.*[9] as a modification of the Flory–Fox equation[10] to compensate for the increasing number of end groups in dendrimer generations (where n_e = number of polymer end groups; M = molecular weight). Several reports have shown that a more classical $1/M$ relationship is valid for particular dendrimers. In general, it appears agreed that the observed dendrimer T_g reaches a plateau at high generation.[11a,11b]

Herein we report the synthesis of a systematic range of polyurethane dendrons and dendrimers, from generation one to four, with three different surface functionalities and two different core molecules (aromatic and aliphatic). These twenty-six new materials have been investigated using differential scanning calorimetry (DSC) to establish trends in T_g and dendrimer structure. Comparisons are presented that utilise the Flory–Fox equation in its classical form and the generally accepted corrected equation that accounts for the unusual number of end groups inherent in dendrimers, suggesting that the modified Flory–Fox equation is unnecessary. We also derive a new and simplified equation relating T_g purely to structural and repeating mass features of the dendrimer and demonstrate that the accepted modifications of the Flory–Fox equation relate directly to a classical 1/M relationship for T_g.

Experimental

Materials

Starting materials were purchased from Aldrich, Acros, Lancaster and Raylo Chemicals, Canada (CDI) and used without further purification. Toluene and benzene were analytical grade and were used as received. The ethanol used was general purpose solvent grade. All reactions were performed under an atmosphere of N_2, unless stated otherwise. Silica gel used for column chromatography was supplied from Aldrich (70–270 mesh, 60 Å) or Fluorochem (40–63u, 60 Å). For preparative gel permeation chromatography, BioBeads ®, S-X1 Beads purchased from Bio-Rad were used in a column mode.

Methods

Elemental analysis data was obtained from an Exeter Analyser CE-440. NMR spectra were recorded using either a Varian Mercury-200 (^{1}H at 200 MHz and ^{13}C at 50.2 MHz), a Bruker AM-250 (^{1}H at 250.1 MHz and ^{13}C at 62.9 MHz), a Varian Unity-300 (^{1}H at 299.9 MHz and ^{13}C at 75.4 MHz), a Varian Mercury 400 (^{1}H at 400 MHz and ^{13}C at 100 MHz) or a Varian Inova-500 (^{1}H at 500 MHz and ^{13}C at 125 MHz). Deuterated solvents were used as supplied from Aldrich ($CDCl_3$ and D_2O) and Cambridge Isotope Laboratories (CD_3OD and $(CD_3)_2SO$). Chemical shifts (δ) are reported in parts per million (ppm) with respect to an internal reference of tetramethylsilane (TMS) using residual solvent signals as secondary references.

For gas chromatography electron ionisation (GC-EI) and gas chromatography chemical ionisation (GC-CI) were recorded using Micromass Autospec instruments. Electrospray mass spectra (ES- MS) were obtained on a Micromass LCT instrument. A solution of the sample in dichloromethane of concentration of 1 mg ml^{-1} was diluted in methanol, to give a solution of 10 μg μl^{-1}. This solution was injected using a syringe pump at a flow rate of 10 μl min^{-1}.

Two different MALDI-TOF mass spectrometers were used in the characterisation of some of the macromolecules. Firstly, a Kratos MALDI-IV MALDI-TOF mass spectrometer, and secondly, a Voyager-DE STR MALDI-TOF mass spectrometer. Trans-3-indole acrylic acid at a concentration in solution (THF) of 10 mg ml^{-1} was used as matrix for MALDI-IV experiments. Dendritic polymer solutions of 1–3 mg ml^{-1} were employed. Dendritic polymer and matrix solutions were mixed in a ratio of 1 : 1 by volume and this solution was deposited into a well on the slide. Mass spectra were obtained in linear mode using polyethylene oxide (Polymer Labs) as an external calibrant. When using the MALDI-TOF Voyager, *trans*-3-indole acrylic acid was used as matrix at 10 mg ml^{-1} in either THF or methanol depending on dendritic polymer solubility. Dendritic polymer solution concentrations varied from 1–3 mg ml^{-1}. Initially, the matrix solution was deposited on the slide, followed by the dendritic solution. Mass spectra were obtained in reflection mode using polyethylene oxide (Polymer Labs) as external calibrants. Some spectra were obtained in linear mode for comparison.

Analysis by GPC was achieved using tetrahydrofuran (THF) as eluent using a flow rate of 1 ml min^{-1} at 30 °C. Columns consisted of 2 × 'mixed B' columns containing PL-gel beads. The columns were calibrated with polystyrene standards (Polymer Laboratories) and samples analysed using conventional calibration with all data collected from a refractive index detector. Differential scanning calorimetry (DSC) was conducted using a Perkin Elmer Pyris 1 DSC calibrated using 99.9% cyclohexane and Indium metal. Samples were heated at a rate of 10 °C per minute from −180 °C to 170 °C, cooled at a rate of 50 °C per minute and heated a second time through the same temperature range at 10 °C per minute. T_g was measured as the midpoint of the inflection of a plot of heat flow *vs.* temperature on the second heating cycle. Melting points were obtained using an Electrothermal IA9200 series digital melting apparatus.

Typical synthesis of imidazole carboxylic esters of alcohols 4-heptanol (1a), *t*-butanol (1b) and cyclohexanol (1c). In a round bottom, glass flask with a reflux condenser attached, a solution of **1b** (6.38 g, 86.1 mmol) in toluene (100 mL) was prepared at room temperature. To this stirred solution was added CDI (16.7 g, 103.1 mmol) and the reaction mixture was heated at 60 °C for 6 h. The solvent was removed using a rotary evaporator and the oil obtained redissolved in CH_2Cl_2 (200 ml). The organic phase was washed with water (3 × 200 ml), dried over $MgSO_4$, filtered and the solvent removed *in vacuo*. The product was dried under vacuum (10^{-1} mbar, 1 day), to yield the imidazole carboxylic ester as a white crystalline solid (13.7 g, 95%). Found C 56.89; H 7.16; N 16.58%. Calculated for $C_8H_{12}N_2O_2$, C 57.13; H 7.19; N 16.66%. ^{13}C NMR (62.9MHz, $CDCl_3$) δ (ppm) = 27.6, 85.33, 116.9, 130.0, 136.8, 146.9. ^{1}H NMR (300 MHz, $CDCl_3$) δ (ppm) = 1.64 (s,9H), 7.07 (s,1H), 7.4 (s,1H), 8.13 (s,1H). T_m = 51 °C.

Using ***1c****.* Yield was a pale yellow oil (93%). Found C 62.49; H 8.60; N 13.23%. $C_{11}H_{18}N_2O_2$ requires, C 62.83; H 8.63; N 13.32%. ^{13}C NMR (62.8 MHz, $CDCl_3$) δ (ppm) = 13.0, 18.4, 36.0, 79.7, 117.1, 130.3, 137.0, 149.0. ^{1}H NMR (300 MHz, $CDCl_3$) δ (ppm) = 0.95 (t, J = 7.2 Hz,6H), 1.41 (m,4H), 1.69 (m,4H), 5.11 (qn, J = 6.2 Hz,1H), 7.08 (m,1H), 7.43 (t, J = 1.2 Hz,1H), 8.15 (s,1H). *m/z* (GC, EI) 210 $[M + H]^+$, calc. M_w = 210.27.

*Using **1a***. Yield was a white crystalline solid (88%). Found C 61.83; H 7.33; N 14.32%. $C_{10}H_{14}N_2O_2$ requires, C 61.84; H 7.26; N 14.42%. ^{13}C NMR (62.9 MHz, $CDCl_3$) δ (ppm) = 23.4, 25.0, 31.2, 77.7, 117.1, 130.0, 136.9, 147.9. ^{1}H NMR (200 MHz, $CDCl_3$) δ (ppm) = 1.39–1.65 (m,6H), 1.79 (m,2H), 1.98 (m,2H), 5.01 (m,1H), 7.08 (s,1H), 7.44 (s,1H), 8.15 (s,1H). *m/z* (GC, EI) 194 $[M + H]^+$, calc. M_w = 194.23.

Typical selective synthesis of amine functional dendrons 2a, 2b, 2c. The imidazole carboxylic ester of **1a** (33.0 g, 156.9 mmol) was dissolved in toluene (250 ml) and diethylenetriamine (9.32 g, 90.3 mmol) added to the solution. The mixture was stirred and heated at 60 °C for 16 h. The solvent was removed under reduced pressure and the mixture redissolved in CH_2Cl_2 (150 ml). The organic phase was washed with distilled water (4 × 150 ml), dried over $MgSO_4$ and after filtration the solvent was removed *in vacuo*. The colorless oil obtained was dried under vacuum (10^{-1} mbar) to give **2a** as a white waxy solid (26.2 g, 86%). Found C 61.82; H 10.72; N 10.65%. $C_{20}H_{41}N_3O_4$ requires C 61.98; H 10.66; N 10.84%. ^{13}C NMR (100 MHz, $CDCl_3$) δ (ppm) = 14.0, 18.5. 36.6, 40.6, 48.8, 74.4, 157.0. ^{1}H NMR (400 MHz, $CDCl_3$) δ (ppm) = 0.91 (t, J = 7.2 Hz,12H), 1.40 (m,8H), 1.48 (m, 8H), 2.76 (t, J = 5.2 Hz,4H), 3.27 (m,4H), 4.77 (qn, J = 5.6 Hz,2H), 5.01 (s, br, O(CO)N*H*CH_2). *m/z* (GC, EI) 388 $[M + H]^+$, calc. M_w = 387.56.

*Using the imidazole carboxylic ester of **1b***. **2b** was a white crystalline solid (118.0 g, 77%). Found C 54.63; H 9.52; N 13.34%. Calculated for $C_{14}H_{29}N_3O_4$, C 55.42; H 9.63; N 13.85%. ^{13}C NMR (62.9 MHz, $CDCl_3$) δ (ppm) = 28.4, 40.3, 48.8, 79.7, 156.1. ^{1}H NMR (300 MHz, $CDCl_3$) δ (ppm) = 1.35 (s, br, CH_2N*H*CH_2), 1.43 (s,18H), 2.71 (t, J = 5.7 Hz,4H), 3.20 (m,4H), 4.99 (s, br, O(CO)N*H*CH_2); on addition of a drop of D_2O the signals corresponding to the N–H resonances of the urethane and secondary amine functions disappear. *m/z* (ES MS) 304 $[M + H]^+$, 326 $[M + Na]^+$, doubly charged adduct 629 $[2M + Na]^+$, calc. M_w = 303.40. T_m = 71 °C.

*Using the imidazole carboxylic ester of **1c***. **2c** was as a white crystalline solid (76%). T_m = 58 °C. Found C 60.32; H 9.37; N 11.71%. $C_{18}H_{33}N_3O_4$ requires, C 60.82; H 9.36; N 11.82%. ^{13}C NMR (100 MHz, $CDCl_3$) δ (ppm) = 23.9, 25.3, 32.0, 40.5, 48.7, 73.0, 156.5. ^{1}H NMR (400 MHz, $CDCl_3$) δ (ppm) = 1.23–1.56 (m, 12H), 1.71 (m,4H), 1.87 (m,4H), 2.76 (t, J = 6 Hz,4H), 3.27 (m,4H), 4.63 (m,2H), 5.05 (s, br, O(CO)N*H*CH_2). *m/z* (ES MS) 356 $[M + H]^+$, 378 $[M + Na]^+$, doubly charged adducts 711 $[2M + H]^+$, 733 $[2M + Na]^+$, calc. M_w = 355.47.

Typical synthesis of OH functional first generation dendrons 3a, 3b, 3c. To a stirred solution of **2a** (26.2 g, 67.5 mmol) in ethanol (200 ml), propylene oxide (11.8 g, 202 mmol) was added and the mixture heated at 30 °C for 20 h. Solvent was removed using the rotary evaporator and the oil dried under vacuum (10^{-1} mbar, 1day). Purification by column chromatography (silica gel, eluting with EtOAc) gave **3a** as a colourless oil (23.8 g, 91%). T_g = −39.5 °C. Found C 61.90; H 10.61; N 9.43%. $C_{23}H_{47}N_3O_5$ requires, C 61.99; H 10.63; N 9.43%. ^{13}C NMR (62.9 MHz, $CDCl_3$) δ (ppm) = 14.0, 18.5, 20.0, 36.7, 39.2, 55.1, 63.2, 64.1, 74.4, 157.2. ^{1}H NMR (300 MHz, $CDCl_3$) δ (ppm) = 0.91 (t, J = 7.2 Hz,12H), 1.12 (d, J = 6.3 Hz,3H), 1.33 (m,8H), 1.47 (m,8H), 1.63 (s, br, O*H*), 2.34 (dd, J = 12.9 Hz, J = 9.9 Hz,1H), 2.46 (dd, J = 13.2 Hz, J = 3 Hz,1H), 2.56 (dt, J = 13.2 Hz, J = 5.4 Hz,2H), 2.67 (m, 2H), 3.23 (m,4H), 3.73 (m,1H), 4.76 (qn, J = 6 Hz,2H), 5.07 (s, br, O(CO)N*H*CH_2). *m/z* (GC, EI) 446 $[M + H]^+$, calc. M_w = 445.64.

*Using **2c***. **3c** was a sticky colourless oil (86%). T_g = 2.0 °C. Found C, 60.15; H 9.42; N, 9.67%. $C_{21}H_{39}N_3O_5$ requires, C 60.99; H 9.51; N 10.16%. ^{13}C NMR (62.9 MHz, $CDCl_3$) δ (ppm) = 19.8, 23.6, 25.2, 31.8, 39.2, 54.9, 63.1, 63.9, 72.7, 156.7. ^{1}H NMR (300 MHz, $CDCl_3$) δ (ppm) = 1.12 (d, J = 6.4 Hz,3H), 1.25 (m,10H), 1.52 (m,2H), 1.72 (m,4H), 1.86 (m,4H), 2.33 (dd, J = 12.9 Hz, J = 9.3 Hz,2H), 2.42 (dd, J = 13.1 Hz, J = 3 Hz,2H) 2.52 (dt, J = 13.2 Hz, J = 4.8 Hz,2H), 2.69 (m,2H), 3.22 (m,4H), 3.72 (m,1H), 4.62 (m,2H), 5.17 (s, br, O(CO)N*H*CH_2). *m/z* (GC CI) 414 $[M + H]^+$, calc. M_w = 413.55.

*Using **2b***. **3b** was a white crystalline solid (89%). T_g = −18 °C, T_m = 61.8 °C (first heating run); T_g = −5 °C (second run). Found C 56.21; H 9.82; N 11.57%. $C_{17}H_{35}N_3O_5$ requires, C 56.49; H 9.76; N 11.62%. ^{13}C NMR (62.9 MHz, $CDCl_3$) δ (ppm) = 20.0, 28.3, 38.7, 55.1, 63.0, 63.9, 79.3, 156.5. ^{1}H NMR (300 MHz, $CDCl_3$) δ (ppm) = 1.12 (d, J = 6.3 Hz,3H), 1.46 (s,18H), 2.37 (m,2H), 2.50 (dt, J = 13.2 Hz, J = 4.5 Hz,2H), 2.68 (m,2H), 3.19 (m,4H), 3.76 (m,1H), 5.13 (s, br, O(CO)N*H*CH_2). *m/z* (GC, EI) 361 $[M + H]^+$, calc. M_w = 361.48.

Synthesis of 1-[*N*,*N*-bis(2-aminoethyl) amino]-2-propanol, 4. 4M HCl/EtOAc (250 mL) was added to a stirred solution of **3b** (55.0 g, 152.3 mmol) in EtOAc (100 ml) at room temperature. On addition of the acid the reaction mixture effervesced and the white suspension formed was stirred for 3 h. The mixture was concentrated *in vacuo* and the orange oil obtained was dried under vacuum to give the tris-ammonium salt of **4** as a pale yellow solid. The tris-ammonium salt was characterized by ^{1}H and ^{13}C NMR spectroscopy; ^{13}C NMR (62.9 MHz, D_2O) δ (ppm) = 22.6, 36.5, 53.4, 62.7, 64.5 and ^{1}H NMR (200MHz, D_2O) δ (ppm) = 1.26 (d, J = 6.4 Hz,3H), 3.21 (dd, J = 13.6 Hz, J = 10.4 Hz,1H), 3.35 (dd, J = 13.6 Hz, J = 3 Hz,1H), 3.48 (m,4H), 3.62 (m,4H), 4.23 (m,1H). Amberlite ® ion exchange beads (700g) were activated by stirring the beads in a 2M KOH solution in distilled water (300 mL) for 1 h. The beads were subsequently isolated by filtration and washed with distilled water (1000 ml). The tris-ammonium salt of **4** was dissolved in distilled water (150 ml) and added to a beaker (1000 ml) containing activated ion exchange beads in distilled water. The beads and solution were stirred for 4 h and the mixture filtered. The filtrate was concentrated using the rotary evaporator and the oil obtained was stirred and dried under vacuum to give a pale yellow solid. It was necessary to repeat the ion exchange process, so after the reactivation of the beads the procedure was repeated using the pale yellow solid. After this second ion exchange process, a yellow oil was isolated. The oil was purified by vacuum distillation (10^{-1} mbar, 160 °C) to give **4** as a colourless oil (15.7 g, 64%). ^{13}C NMR (62.9 MHz, $CDCl_3$) δ (ppm) = 19.9, 39.8, 57.8, 62.8, 64.8. ^{1}H NMR (300MHz, $CDCl_3$) δ (ppm) = 1.10 (d, J = 6.3 Hz,3H), 2.32 (dd, J = 13.2 Hz, J = 9.9 Hz,1H), 2.44 (dd, J = 13.2 Hz, J = 2.7 Hz,1H), 2.58 (m,4H), 2.76 (m,4H), 3.79 (m,1H). *m/z* (GC, EI) 162.6 $[M + H]^+$, calc. M_w = 161.25.

Typical synthesis of OH functional second generation dendrons 5a, 5b, 5c. CDI (4.55 g, 28.1 mmol) was added to a stirred solution of **3b** (8.82 g, 24.4 mmol) in toluene (100 ml). The mixture was heated at 60 °C for 6 h. Subsequently, the reaction mixture was analysed by ^{1}H NMR spectroscopy and interpretation of the spectrum indicated there was no evidence of the starting materials. **4** (2.17 g, 13.4 mmol) was added and the solution was heated for 20 h. The reaction mixture was concentrated *in vacuo* and redissolved in CH_2Cl_2 (200 ml). The organic phase was subsequently washed with water (3 × 250 ml), dried over $MgSO_4$ and the solvent removed using a rotary evaporator. The resulting pale yellow oil was purified by column chromatography (silica gel, eluting with EtOAc:C_6H_{12} 3 : 2) and the colourless oil obtained was dried under vacuum (10^{-1} mbar) to give **5b** as a colourless amorphous solid (5.7 g, 50%). T_g = 25 °C. Found C 54.62; H 9.14; N 13.50%. $C_{43}H_{85}N_9O_{13}$ requires, C 55.17; H 9.15; N 13.47%. ^{13}C NMR (400 MHz, CD_3OD, 50 °C) δ (ppm) = 18.9, 21.0, 28.9, 39.9, 40.2, 55.7, 56.0, 61.1, 64.1, 66.2, 71.0, 80.1, 158.3, 158.8. 66.2 ppm is split into three peaks – 66.25, 66.18, 66.12 – with relative intensities 1: 2.0: 0.8. ^{1}H NMR (500 MHz, CD_3OD) δ (ppm) = 1.12 (d, J = 6.0 Hz,3H, $CH_2CH(OH)C\mathit{H}_3$), 1.19 (d, J = 6.5 Hz,6H, $C(H)(C\mathit{H}_3)OC(O)N(H)$), 1.40 (s,36H, $C(O)C(C\mathit{H}_3)$), 2.41 (m,2H, $NC\mathit{H}_2CH(CH_3)(OH)$), 2.49 & 2.66 (m,4H, $NC\mathit{H}_2C(H)(CH_3)OC(O)N(H)$), 2.58 (m,12H, $O(CO)N(H)CH_2C\mathit{H}_2$), 3.08 (m,12H, $O(CO)N(H)C\mathit{H}_2CH_2$), 3.22 (m,4H, $O(CO)NHC\mathit{H}_2CH_2$), 3.78 (m,1H, $CH_2C\mathit{H}(CH_3)(OH)$), 4.85 (m, obscured by H_2O peak,2H, $CH_2C(\mathit{H})(CH_3)OC(O)N(H)$), 6.43 (s, br, $O(CO)N\mathit{H}CH_2$), 6.88 (s, br,2H, $O(CO)N\mathit{H}CH_2$). *m/z* (ES MS) 936 $[M + H]^+$, 958 $[M + Na]^+$, 974 $[M + K]^+$, 469 $[M + H]^{2+}$, 480 $[M + Na]^{2+}$, 488 $[M + K]^{2+}$, 491 $[M + 2Na]^{2+}$, calc. M_w = 936.19. GPC; M_w = 1120, PDI = 1.02.

*Using **3a**.* Purification was achieved by column chromatography (silica gel, eluting with EtOAc:C_6H_{12} 1 : 2) to give **5a** as a sticky colourless oil (49%). T_g = −4 °C. Found C 59.54; H 9.91; N 11.20%. $C_{55}H_{109}N_9O_{13}$ requires, C 59.81; H 9.95; N 11.41%. ^{13}C NMR (62.9 MHz, CD_3OD) δ (ppm) = 14.5, 18.9, 19.5, 20.9, 37.8, 39.9 (resonances from two distinct carbons overlap), 55.5, 55.9, 60.9, 64.0, 65.8 (split into 3 peaks), 70.6, 74.9, 158.6, 158.9. ^{1}H NMR (400 MHz, CD_3OD) δ (ppm) = 0.92 (t, J = 7.2 Hz,24H), 1.12 (d, J = 6.4 Hz,3H), 1.19 (d, J = 6.4 Hz,6H), 1.30–1.41 (m,16H), 1.47–1.54 (m,16H), 2.38–2.68 (m,18H), 3.09–3.28 (m,12H), 3.77 (m, 1H), 4.73 (m,4H), 4.85 (m,2H), 6.67 (s, br, $O(CO)N\mathit{H}CH_2CH_2$), 6.89 (s, br, $O(CO)N\mathit{H}CH_2CH_2$). *m/z* (ES MS) 1105 $[M + H]^+$, 1127 $[M + Na]^+$, 1143 $[M + K]^+$, 553 $[M + H]^{2+}$, 564 $[M + Na]^{2+}$, 575 $[M + 2Na]^{2+}$. *m/z* (MALDI-TOF (Kratos) MS) 1105 $[M + H]^+$, 1127 $[M + Na]^+$, calc. M_w = 1104.51. GPC; M_w = 1180, PDI = 1.01.

*Using **3c**.* **5c** was a colourless oil (42%). T_g = 30 °C. Found C 58.62; H 8.97; N 11.98%. $C_{51}H_{93}N_9O_{13}$ requires, C 58.88; H 9.01; N 12.12%. ^{13}C NMR (62.8 MHz, CD_3OD) δ (ppm) = 18.9, 21.0, 24.8, 26.5, 33.1, 39.9 (resonances from two distinct carbons overlap), 55.5, 55.9, 60.9, 64.0, 66.0 (split into 3 peaks), 70.7, 74.0, 158.6, 158.8. ^{1}H NMR (400 MHz, CD_3OD) δ (ppm) = 1.12 (d, J = 6 Hz,3H), 1.18 (d, J = 6 Hz,6H), 1.21–1.45 (m,20H), 1.56 (m, 4H), 1.74 (m,8H), 1.85 (m,8H), 2.40–2.70 (m,18H), 3.08–3.27 (m, 12H), 3.78 (m,1H), 4.56 (m,4H), 4.84 (m,2H), 6.61 (s, br, $O(CO)N\mathit{H}CH_2CH_2$), 6.88 (s, br, $O(CO)N\mathit{H}CH_2CH_2$). *m/z* (ES MS) 1040.4 $[M + H]^+$, 1062.4 $[M + Na]^+$, 1078 $[M + K]^+$, 521 $[M + H]^{2+}$, 532 $[M + Na]^{2+}$, 539 $[M + K]^{2+}$, 543 $[M + 2Na]^{2+}$. *m/z* (MALDI-TOF (Kratos) MS) 1041 $[M + H]^+$, 1063 $[M + Na]^+$, 1079 $[M + K]^+$, calc. M_w = 1040.34. GPC; M_w = 970, PDI = 1.02.

Synthesis of third and fourth generation OH functional dendrons 6a, 6b, 6c, 7c. See electronic supporting information (ESI†).

Typical synthesis of first generation dendrimers with aliphatic urethane cores. CDI (5.5 g, 33.9 mmol) was added to a stirred solution of **3b** (10.2 g, 28.3 mmol) in toluene (150 ml). The mixture was heated at 60 °C for 4 h. Subsequently, the reaction mixture was analysed by ^{1}H NMR spectroscopy and interpretation of the spectrum indicated there was no evidence of the starting materials. Tris(2-aminoethyl) amine (1.38 g, 9.42 mmol) was added and the solution was heated at 60 °C for 24 h. The reaction mixture was concentrated *in vacuo* and redissolved in CH_2Cl_2 (150 ml). The organic phase was subsequently washed with water (3 × 150 ml), dried over $MgSO_4$ and the solvent removed by rotary evaporation. The crude product was purified by column chromatography (silica gel, eluting with EtOAc:C_6H_{12}, 1 : 1 increasing to EtOAc) to give G1-*t*-butyl-TAEA as a colourless amorphous solid (3.7 g, 30%). T_g = 38 °C. Found C 55.72; H 8.96; N 13.37%. $C_{60}H_{117}O_{18}N_{13}$ requires, C 55.07; H 9.01; N 13.91%. ^{13}C NMR (100 MHz, CD_3OD at 50 °C) δ (ppm) = 19.0, 28.9, 39.7, 40.1, 55.2, 55.6, 61.0, 70.7, 79.8, 158.1, 158.5. ^{1}H NMR (400 MHz, CD_3OD) δ (ppm) = 1.20 (d, J = 6.4 Hz,9H), 1.44 (s,54H), 2.50 (dd, J = 13.6 Hz, J = 4.8 Hz, 3H), 2.57–2.63 (m, 21H), 3.04–3.25 (m,18H), 4.85 (m,3H) 6.43 (s, br, $O(CO)N\mathit{H}$ CH_2CH_2), 6.79 (s, br, $O(CO)N\mathit{H}CH_2CH_2$). *m/z* (TOF MS ES) 1307 $[M + H]^+$, 1313 $[M + Li]^+$, 1329 $[M + Na]^+$, 676 $[M + 2Na]^{2+}$. *m/z* (MALDI TOF (Kratos) MS) 1307 $[M + H]^+$, 1330 $[M + Na]^+$, 1346 $[M + K]^+$, calc. M_w = 1308.65. GPC; M_w = 1780, PDI = 1.01.

*Using **3a**.* The crude product was purified by column chromatography (silica gel, eluting with EtOAc:C_6H_{12}, 3 : 1 increasing to EtOAc) to give G1-heptyl-TAEA as a colourless solid (32%). T_g = 7 °C. Found C 59.78; H 9.91; N 11.73%. $C_{78}H_{153}O_{18}N_{13}$ requires, C 60.01; H 9.88; N 11.66%. ^{13}C NMR (62.9 MHz, CD_3OD) δ (ppm) = 14.5, 19.0, 19.6, 37.9, 40.0, 55.3, 55.6, 61.0, 70.7, 75.2, 158.7, 159.2. ^{1}H NMR (400 MHz, CD_3OD) δ (ppm) = 0.92 (t, J = 7.2 Hz,36H), 1.20 (d, J = 6 Hz,9H), 1.36 (m,24H), 1.50 (m,24H), 2.50–2.63 (m,24H), 3.10–3.21 (m, 18H), 4.73 (m,6H), 4.86 (m, obscured by H_2O peak,3H), 6.66 (s, br, $O(CO)N\mathit{H}CH_2CH_2$), 6.79 (s, br, $O(CO)N\mathit{H}CH_2CH_2$). *m/z* (ES MS) 1561.1 $[M + H]^+$, 1583.0 $[M + Na]^+$, 781.3 $[M + H]^{2+}$, 792.3 $[M + Na]^{2+}$, 803.3 $[M + 2Na]^{2+}$. *m/z* (MALDI TOF (Voyager) MS) 1561.2 $[M + H]^+$, 1583.1 $[M + Na]^+$. *m/z* (MALDI TOF (Kratos) MS) 1557 $[M + H]^+$, 1580 $[M + Na]^+$, calc. M_w = 1561.13. GPC; M_w = 1740, PDI = 1.02.

*Using **3c**.* The crude product was purified by column chromatography (silica gel, eluting with EtOAc increasing to EtOAc: MeOH 100 : 5) to give G1-cyclohexyl-TAEA as a colourless solid (32%). T_g = 39 °C. Found C 58.30; H 8.73; N 12.06%. $C_{72}H_{129}O_{18}N_{13}$ requires, C 59.03; H 8.88; N 12.43%. ^{13}C NMR (62.9 MHz, CD_3OD) δ (ppm) = 19.0, 24.9, 26.6, 33.2, 40.0, 55.3,

55.5, 61.0, 70.8, 74.0, 158.7, 158.9. ^{1}H NMR (400 MHz, CD_3OD) δ (ppm) = 1.19 (d, J = 4.8 Hz,9H), 1.28–1.40 (m, 30H), 1.54 (m,6H), 1.75 (m,12H), 1.85 (m,12H), 2.49–2.61 (m, 24H), 3.16 (m,18H), 4.56 (m,6H), 4.85 (m, obscured by H_2O peak,3H), 6.60 (s, br, O(CO)N*H*CH_2CH_2), 6.77 (s, br, O(CO)N*H* CH_2CH_2). *m/z* (ES MS) 1464.8 [M + H]$^+$, 1486.7 [M + Na]$^+$, 732.9 [M/2 + H]$^+$, 743.9 [M/2 + Na]$^+$, 755.4 [M/2 + K]$^+$. *m/z* (MALDI TOF (Voyager) MS) 1464.9 [M + H]$^+$, 1486.9 [M + Na]$^+$, 1502.9 [M + K]$^+$, calc. M_w = 1464.87. GPC; M_w = 1350, PDI = 1.02.

Typical synthesis of first generation dendrimers with aromatic ester cores. A solution of **3b** (2.0 g, 5.54 mmol) and 4-dimethylaminopyridine **DMAP** (1.8 g, 14.8 mmol) in benzene (100 ml) was refluxed for 3 h with a Dean–Stark trap filled with molecular sieves attached. The mixture was cooled to room temperature and 1,3,5-benzenetricarbonyl trichloride (0.45g, 1.70 mmol) was added. The reaction mixture was stirred and heated at 40 °C for 3 h and then concentrated *in vacuo*. The crude product obtained was purified by column chromatography (silica gel, eluting with EtOAc:C_6H_{12}, 5 : 1) to give G1-*t*-butyl-BTT as a white amorphous solid (1.75 g, 83%). T_g = 35 °C. Found C 57.08; H 8.45; N 9.86%. $C_{60}H_{105}O_{18}N_9$ requires, C 58.09; H 8.53; N 10.16%. ^{13}C NMR (62.9 MHz, $CDCl_3$) δ (ppm) = 18.1, 28.3, 38.3, 54.6, 59.2, 70.8, 78.9, 131.5, 134.3, 156.1, 164.4. ^{1}H NMR (250 MHz, $CDCl_3$) δ (ppm) = 1.32–1.36 (m,63H), 2.58–2.79 (m,18H), 3.04–3.25 (m,12H), 5.18 (s, br, OC(O) N*H*CH_2), 5.21 (m, 3H), 8.78 (s, 3H). *m/z* (MALDI TOF (Kratos) MS) 1240 [M + H]$^+$, 1263 [M + Na]$^+$, 1280 [M + K]$^+$, calc. M_w = 1240.53. GPC; M_w = 1320, PDI = 1.01.

Using ***3a***. Crude product was purified by column chromatography (silica gel, eluting with EtOAc:C_6H_{12}, 3 : 2) to give G1-heptyl-BTT as a waxy white solid (75%). T_g = −2 °C. Found C 62.53; H 9.61; N 8.33%. $C_{78}H_{141}O_{18}N_9$ requires, C 62.75; H 9.52; N 8.44%. ^{13}C NMR (62.9 MHz, CD_3OD) δ (ppm) = 14.5, 18.6, 19.6, 37.9, 39.9, 55.5, 60.7, 72.2, 75.2, 133.1, 135.3, 159.1, 165.7. ^{1}H NMR (250 MHz, CD_3OD) δ (ppm) = 0.90 (t, J = 7 Hz,36H), 1.25–1.47 (m,57H), 2.65–2.91 (m,18H), 3.18 (m, 12H), 4.68 (m,6H), 5.23 (m,3H), 6.53 (s, br, OC(O)N*H*CH_2), 8.83 (s,3H). *m/z* (MALDI TOF (Kratos) MS) 1490 [M + H]$^+$. *m/z* (MALDI TOF (Voyager) MS) 1493.2 [M + H]$^+$, 1515.2 [M + Na]$^+$, 1531.0 [M + K]$^+$, calc. M_w = 1493.00. GPC; M_w = 1720, PDI = 1.01.

Using ***3c***. The crude product was purified by column chromatography (silica gel, EtOAc:C_6H_{12}, 3 : 1) to give G1-cyclohexyl-BTT as a white amorphous solid (78%). T_g = 40 °C. Found C 61.67; H 8.42; N 8.87%. $C_{72}H_{117}O_{18}N_9$ requires, C 61.91; H 8.44; N 9.03%. ^{13}C NMR (62.9 MHz, $CDCl_3$) δ (ppm) = 18.1, 23.7, 25.3, 31.8, 38.6, 54.4, 59.2, 70.7, 72.7, 131.4, 134.3, 156.4, 164.4. ^{1}H NMR (250 MHz, $CDCl_3$) δ (ppm) = 1.29–1.39 (m, 39H), 1.53 (m,6H), 1.64 (m,12H), 1.82 (m,12H), 2.68–2.90 (m, 18H), 3.22 (m,12H), 4.58 (m,6H), 5.20 (s, br, OC(O)N*H*CH_2), 5.26 (m,3H), 8.81 (s,3H). *m/z* (MALDI TOF (Voyager) MS) 1396.8 [M + H]$^+$, 1418.8 [M + Na]$^+$, 1434.8 [M + K]$^+$. *m/z* (MALDI TOF (Kratos) MS) 1395 [M + H]$^+$, 1417 [M + Na]$^+$, 1433 [M + K]$^+$, calc. M_w = 1396.75. GPC; M_w = 1320, PDI = 1.01.

Synthesis of second and third generation dendrimers with urethane and ester cores. See electronic supporting information (ESI†).

Results and discussion

Synthesis

We have previously reported the synthesis of polyurethane dendrimers using the selective reactions of 1,1′-carbonyl diimidazole derivatives.[6a] In summary, the strategy utilises either a secondary or tertiary alcohol, **1**, as the surface functionality for a convergent dendrimer synthesis, Scheme 1. 4-Heptanol (**1a**), *t*-butanol (**1b**) and cyclohexanol (**1c**) were chosen for the current study to establish differences between highly flexible, sterically bulky and cyclic aliphatic groups.

Each alcohol was reacted with 1,1′-carbonyldiimidazole (CDI) to generate their imidazole carboxylic ester derivatives. Selective reaction of the derivatives with diethylenetriamine led to the formation of the di-urethane products, **2**, without reaction at the secondary amine functionality, as confirmed by mass spectrometry and ^{1}H and ^{13}C nuclear magnetic resonance spectroscopy

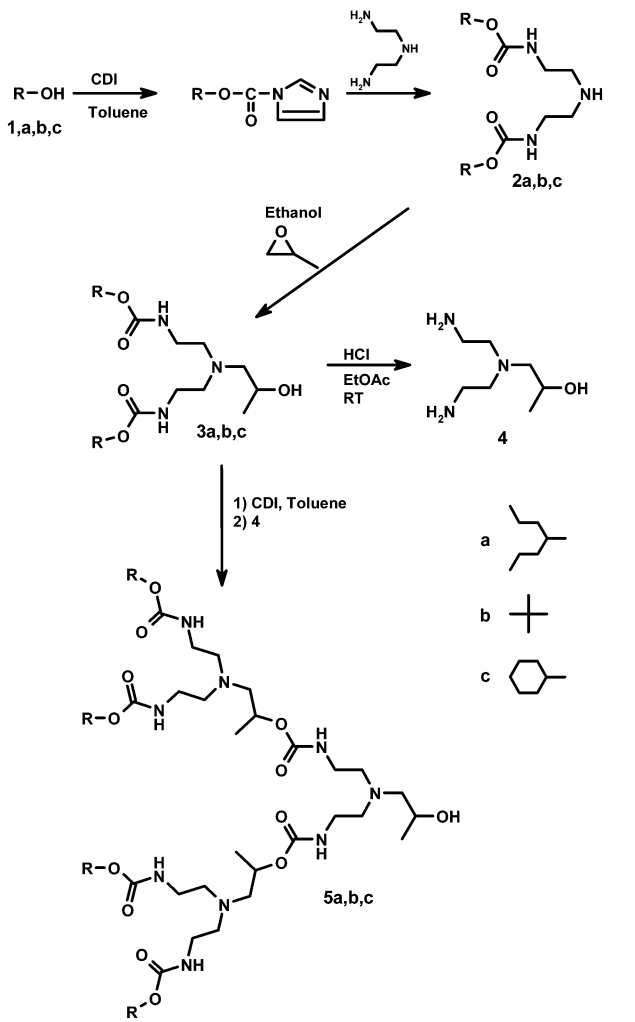

Scheme 1 Selective synthesis of polyurethane dendrimers using 1,1′-carbonyl diimidazole (CDI) derivatives.

(NMR). Ring opening of propylene oxide with **2** generated the first generation dendrons, **3**, bearing a secondary hydroxyl group for subsequent reaction with CDI and formation of imidazole carboxylic ester derivatives. **3b**, derived from the initial reaction of *t*-butanol, was also deprotected to form the triamino alcohol AB_2 branching unit **4**. The imidazole carboxylic esters, from the reaction of **3** with CDI, were reacted with **4** to form larger dendrons. Repetition of this iterative synthesis led to a series of dendrons, shown schematically in Fig. 1.

The generation 1–3 dendrons were coupled, using CDI chemistry, with either tris(2-aminoethyl)amine (TAEA), to form the polyurethane homodendrimer series, or directly with 1,3,5-benzene tricarbonyl trichloride (BTT), forming an aromatic ester core and generating core variability within the series of materials, shown schematically in Fig. 2.

Monitoring of the individual stages of dendron and dendrimer synthesis by ^{1}H and ^{13}C NMR is often hampered at higher generations due to overlapping signals and the inherent structural complexity. The polyurethane materials of this study have an increasing number of chiral carbons generated during the ring opening of propylene oxide. The chiral centres lead to modified chemical environments at the diastereotopic methylene adjacent to the tertiary amine. For the generation 1 dendrons the inequivalence of the methylene protons was readily seen in the ^{1}H NMR spectra as two doublet of doublets due to the germinal and vicinal couplings, exemplified in Fig. 3A and 3B for the 4-heptyl functional generation 1 dendron. The diastereotopic methylene protons of the *t*-butyl functional dendrons were less resolved than the cyclohexyl or 4-heptyl functional materials.

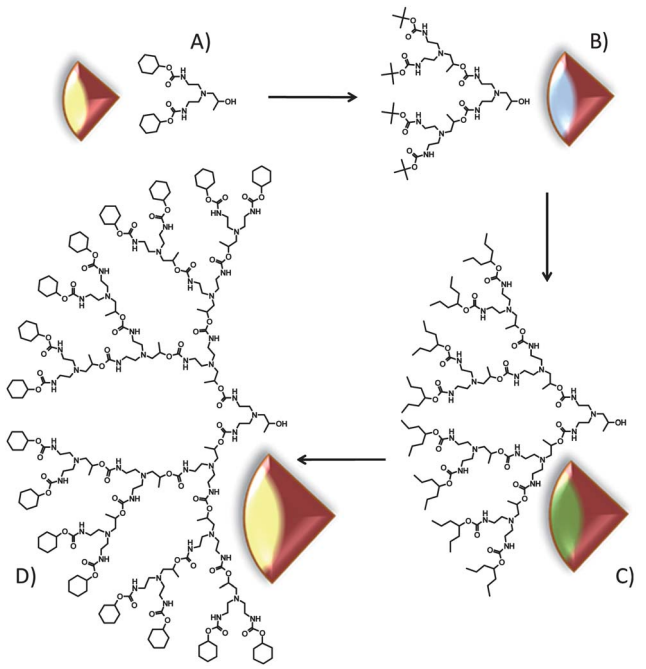

Fig. 1 Schematic representation of generation 1–3 dendron formation. Surface group variation is represented by the coloured wedges (yellow = cyclohexyl, blue = *t*-butyl and green = 4-heptyl). (A) Generation 1 cyclohexyl functional polyurethane dendron, (B) generation 2 *t*-butyl functional polyurethane dendron, (C) gGeneration 3 4-heptyl functional dendron, (D) generation 4 cyclohexyl functional polyurethane dendron.

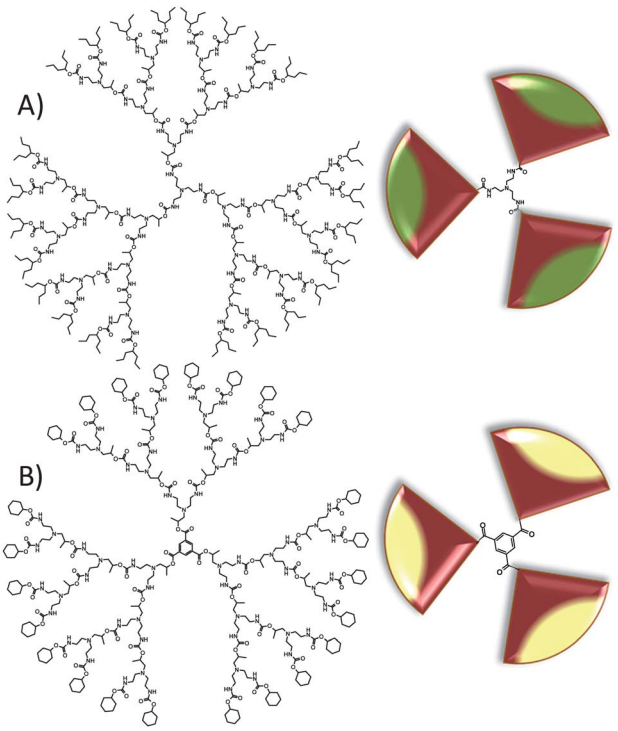

Fig. 2 Generation 3 4-heptyl and cyclohexyl functional polyurethane dendrimers coupled with either (A) tris(2-aminoethyl)amine or (B) 1,3,5-benzene tricarbonyl tichloride cores and schematic representations of the dendrimers.

At generation 2, the dendrons also exhibited a noticeable difference with respect to the shift of the methyl protons in the ^{1}H NMR, shown in Fig. 3C & D for the 4-heptyl generation 2 dendron. Two distinct doublets at approximately $\delta = 1.12$ and 1.18ppm were readily integrated and assigned to the dendron focal point (H_α) and the reacted generation 1 dendron methyls (H_β), adjacent to the urethane groups, respectively. Interestingly, the N–H protons of the six urethane groups of the generation 2 dendrons were also readily seen within the ^{1}H NMR spectra, Fig. 3E, with distinctly different chemical shifts, suggesting different environments. Although the chemical shift of the N–H protons of the two urethane groups near to the focal point (NH_δ) did not vary with different surface functionality ($\delta = 6.88$ppm), the resonance of the internal urethanes (NH_γ) showed a significant shift from $\delta = 6.67$ppm (4-heptyl surface) to $\delta = 6.61$ppm (cyclohexyl surface) and $\delta = 6.43$ppm (*t*-butyl surface). This suggests a hydrogen bonding contribution that decreases with the increasing steric bulk of the surface groups. The *t*-butyl surface may prevent interaction between urethanes at the periphery of the dendrons however the less bulky cyclohexyl, or flexible 4-heptyl, groups appear to allow a close proximity of the urethane groups and subsequent hydrogen bonding.

Analysis of the generation 1 dendrimers, coupled to a TAEA core, by ^{1}H NMR showed an identical chemical shift relationship for the nine urethane N–H protons. The three core urethanes exhibited a single resonance at approximately $\delta = 6.78$ppm for all surface groups however the six peripheral urethane N–H resonances varied from $\delta = 6.66$ppm (4-heptyl surface) to $\delta = 6.60$ppm (cyclohexyl surface) and $\delta = 6.43$ppm (*t*-butyl surface).

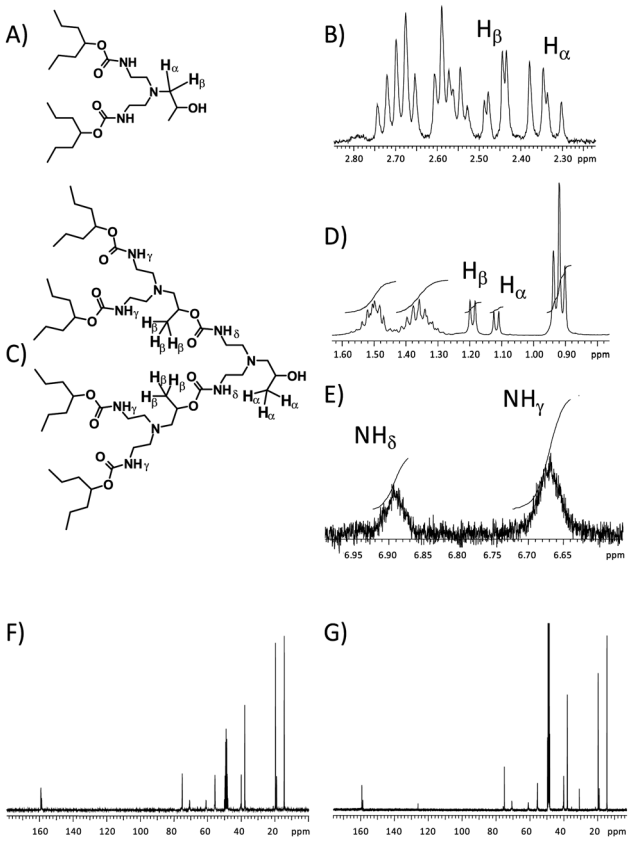

Fig. 3 Indicative ^{1}H and ^{13}C nuclear magnetic resonance spectra for 4-heptyl functional materials; (A) generation 1 dendron, (B) ^{1}H NMR spectrum of the generation 1 dendron ($CDCl_3$), (C) generation 2 dendron, (D&E)^{1}H NMR spectrum of the generation 2 dendron (CD_3OD), (F) ^{13}C NMR spectrum of the generation 3 dendron (CD_3OD), (G) ^{13}C NMR spectrum of the generation 3 dendrimer (CD_3OD) coupled with tris(2-aminoethyl) amine.

Higher generation dendrimers showed considerable overlap and definitive data was difficult to obtain. For example, the generation 3 *t*-butyl functional dendrimer (TAEA core) showed two N–H resonances at $\delta = 6.71$ppm and $\delta = 6.42$ppm, however the signal at $\delta = 6.71$ppm was broad and may correspond to several layers of overlapping signals but the resonance at $\delta = 6.42$ppm is identical to the earlier *t*-butyl functional dendrimers. This suggests the outer layers of the dendrimer do not readily hydrogen bond when this surface group is present however internal layers are able to do so to some degree.

To explore the hydrogen bonding further, generation 1–3 dendrimers with 4-heptyl and *t*-butyl surfaces were studied using solution-phase infrared spectroscopy in CH_2Cl_2, Fig. 4. The N–H stretching frequency, at approximately 3450 cm^{-1}, varies (to lower wavenumber) and broadens when it is involved in hydrogen bonding.[12] Deconvolution of the complicated dual signal from 3200–3500 cm^{-1}, Fig. 4A, allows an approximation of the percentage of hydrogen-bonded urethane groups, after subtraction of the pure solvent spectrum. Each sample was repeated three times to generate an average percentage of hydrogen bonding. The 4-heptyl functional dendrimers, Fig. 4B, showed no meaningful change in hydrogen bonding with increasing generation (generation 1 = 79%, generation 2 = 80%,

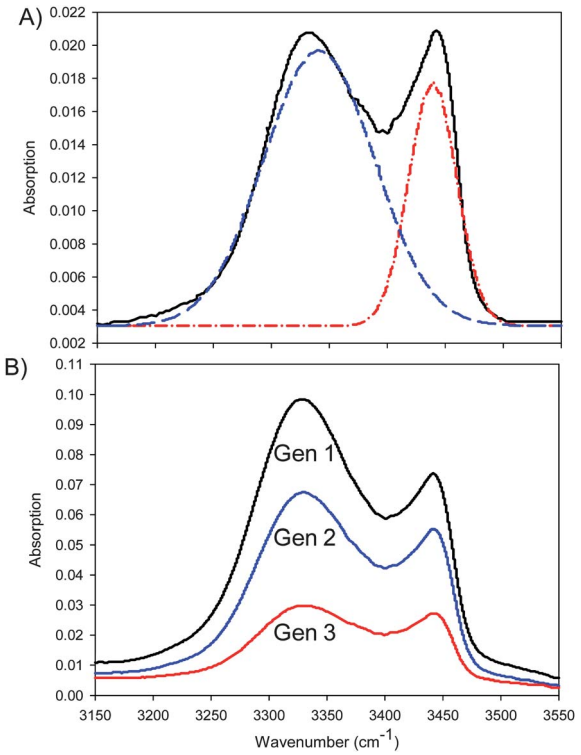

Fig. 4 Solution phase IR spectra of polyurethane dendrimers; (A) *t*-butyl functional generation 1 dendrimer with deconvolution, (B) generation 1–3 4-heptyl functional dendrimers.

generation 3 = 80%) however the *t*-butyl functional dendrimers did show a systematic increase (generation 1 = 73%, generation 2 = 75%, generation 3 = 80%). If 80% involvement of the urethane N–H groups is considered to be a limiting maximum for these structures (based on the 4-heptyl functional dendrimers) it appears that the *t*-butyl groups prevent the urethanes in the peripheral regions of the dendrimers from achieving a proximity that allows the formation of hydrogen bonds at low generation however as dendrimer generation increases, the internal urethane layers are able to hydrogen bond and potentially some peripheral hydrogen bonding is also possible.

Analysis of the ^{13}C NMR spectra again showed complexity derived from the chiral nature of the secondary carbon generated from the ring opening of propylene oxide. When the alcohol is reacted to form a urethane, the carbon resonance was seen at approximately δ = 71ppm as a relatively broad peak. The unreacted *C*–OH at the focal point of each dendron however was seen as split into three separate peaks between $\delta = 66$–66.4ppm in the ratio of approximately 2 : 4 : 1.6 probably due to the ratios of R and S enantiomers and the proximity of the nitrogen atom allowing the potential for interaction with the hydroxyl group. The urethane carbonyl carbon was clearly observed at approximately δ = 157 ppm, Fig. 3F & G, and also displayed splitting which was assigned to the different environments within the various regions of the dendrimer generations. Ester carbonyl peaks at approximately δ = 165 ppm were observed when coupling to BTT. In total twenty-six new dendritic structures were synthesised as part of this study, Fig. 5, however a number of possible structures were omitted to allow focus on, and study of, systematic variations within specific sequences.

Glass transition temperature studies

There have been many studies that have investigated the T_g of dendritic polymers and shown the effect of changing end group chemistry, core chemistry and generation number.[13] Several studies have concluded that the conventional Flory–Fox equation, eqn (1), relating T_g to the reciprocal of molecular weight (1/M), with the intercept correlating to T_g at infinite molecular weight ($T_{g\infty}$), does not fully represent dendrimer behaviour as the number of end-groups within dendritic polymer structures (including the focal point of dendrons) are not insignificant at very high molecular weights.[8,9] Other groups have concluded that the 1/M relationship *is* pertinent to dendritic polymers.[14] Within this study, we have measured the T_g of the polyurethane dendrimers, with TAEA and BTT cores, and dendrons to investigate effects of the systematic change of surface functionality, core chemistry and generation within this new series of dendritic polymers. The data is summarised in Table 1 and consistently shows increasing T_g with generation, as expected. T_g values were distributed from −40 °C to 50 °C and dendrons exhibited a lower T_g than the corresponding dendrimers. Within the dendron series, the flexible 4-heptyl aliphatic surface group generated lower values of T_g than the other more sterically crowded surface groups; cyclohexyl generally produced the highest values. Although the series of aromatic and aliphatic core dendrimers is incomplete, the 4-heptyl surface group yielded the lowest T_g values for both cores however the *t*-butyl surface functionality appears to exhibit higher T_gs than the cyclohexyl functionality above generation 2 when using TAEA as the core molecule. The cyclohexyl group generated the highest T_g values for dendrimers with the rigid aromatic BTT core.

Thermal studies of polyurethane dendrimers

As mentioned above, there have been several reports suggesting that the Flory–Fox equation is not relevant to the prediction of $T_{g\infty}$ for some dendrimers and others that claim direct relevance for other materials. We have analysed this polyurethane dendron/dendrimer series using three approaches; conventional Flory–Fox, modified Flory–Fox (considering number of chain

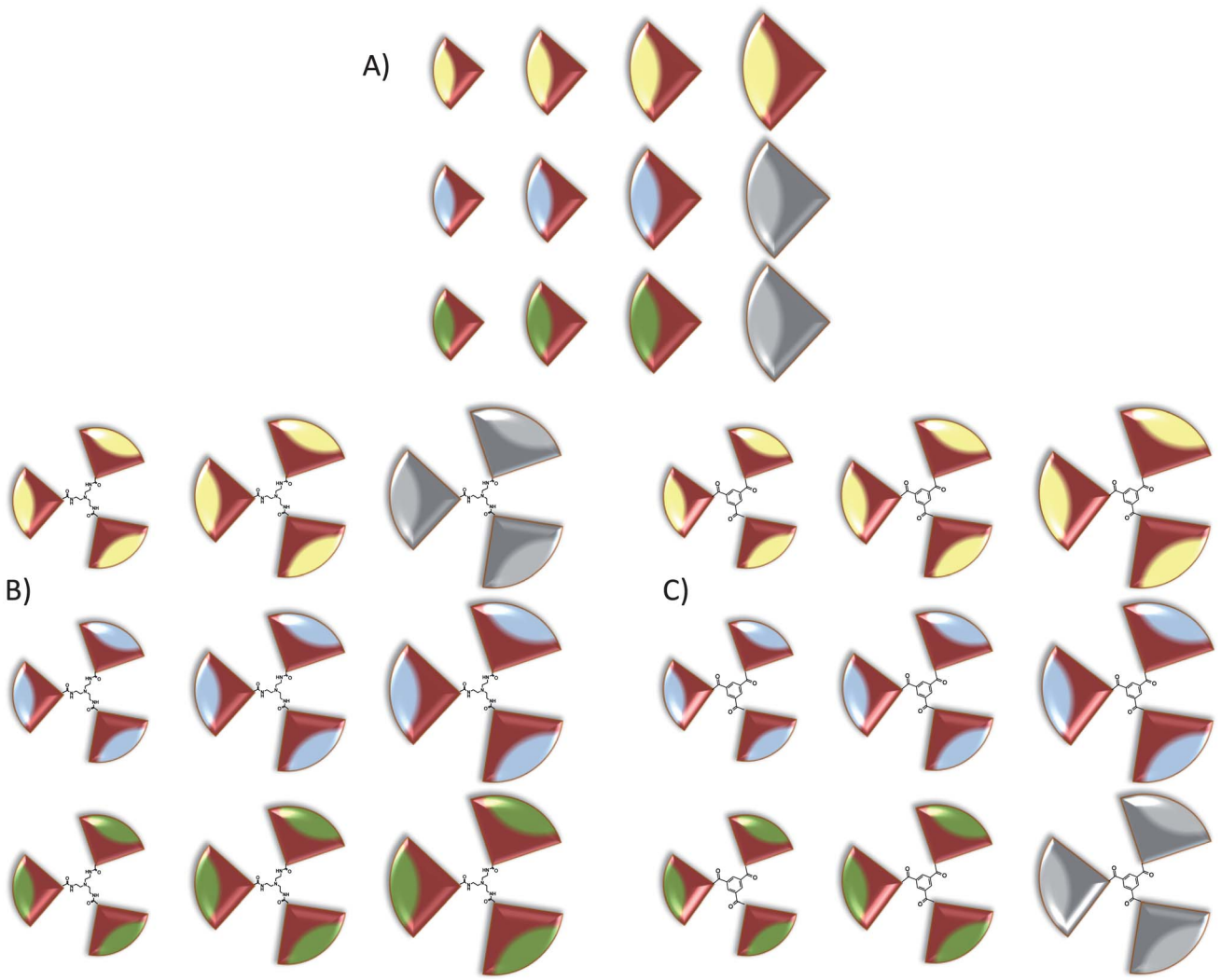

Fig. 5 Schematic representation of polyurethane dendrons and dendrimers within this study. (A) Polyurethane dendrons, (B) polyurethane dendrimers using tris(2-aminoethyl)amine cores and (C) polyurethane dendrimers using 1,3,5-benzene tricarbonyl trichloride cores. KEY: Surface groups - cyclohexyl (yellow), *t*-butyl (blue) and 4-heptyl (green); grey molecules were not synthesised.

Table 1 Experimental and calculated parameters for polyurethane dendrons and dendrimers with varying generation and surface chemistry

Sample	Type	Core	M (g mol^{-1})	n_e	1/M ($Da^{-1} \times 10^{-3}$)	$(n_e/M)-(n_e/M)_\infty$ ($Da^{-1} \times 10^{-3}$)	T_g (°C)	A (Da)	B (Da)	C (Da)
G1-cyclohexyl	Dendron	—	413.56	2	2.418	1.645	2	213.24	200.32	313.40
G2-cyclohexyl	Dendron	—	1040.36	4	0.961	0.654	30	213.24	200.32	313.40
G3-cyclohexyl	Dendron	—	2293.96	8	0.436	0.297	40	213.24	200.32	313.40
G4-cyclohexyl	Dendron	—	4801.16	16	0.208	0.142	48	213.24	200.32	313.40
G1-*t*-butyl	Dendron	—	361.49	2	2.766	2.053	−6	213.24	148.25	287.37
G2-*t*-butyl	Dendron	—	936.21	4	1.068	0.793	25	213.24	148.25	287.37
G3-*t*-butyl	Dendron	—	2085.66	8	0.479	0.356	40	213.24	148.25	287.37
G1-4-heptyl	Dendron	—	445.65	2(4)[a]	2.244	1.452(2.905)[a]	−40	213.24	232.41	329.45
G2-4-heptyl	Dendron	—	1104.53	4(8)[a]	0.905	0.586(1.172)[a]	-4	213.24	232.41	329.45
G3-4-heptyl	Dendron	—	2422.31	8(16)[a]	0.413	0.267(0.5344)[a]	11	213.24	232.41	329.45
G1-cyclohexyl	Dendrimer	TAEA	1464.91	6	0.683	0.905	39	415.49	1049.42	940.20
G2-cyclohexyl	Dendrimer	TAEA	3345.31	12	0.299	0.396	44	415.49	1049.42	940.20
G1-*t*-butyl	Dendrimer	TAEA	1308.68	6	0.764	1.105	38	415.49	893.19	862.09
G2-*t*-butyl	Dendrimer	TAEA	3032.85	12	0.330	0.477	47	415.49	893.19	862.09
G3-*t*-butyl	Dendrimer	TAEA	6481.19	24	0.154	0.223	49	415.49	893.19	862.09
G1-4-heptyl	Dendrimer	TAEA	1561.17	6(12)[a]	0.641	0.808(1.616)[a]	7	415.49	1145.69	988.34
G2-4-heptyl	Dendrimer	TAEA	3537.82	12(24)[a]	0.283	0.356(0.713)[a]	17	415.49	1145.69	988.34
G3-4-heptyl	Dendrimer	TAEA	7491.14	24(48)[a]	0.168	0.168(0.337)[a]	19	415.49	1145.69	988.34
G1-cyclohexyl	Dendrimer	BTT	1396.78	6	0.716	1.105	40	483.61	913.17	940.20
G2-cyclohexyl	Dendrimer	BTT	3277.19	12	0.305	0.471	48	483.61	913.17	940.20
G3-cyclohexyl	Dendrimer	BTT	7037.99	24	0.142	0.219	50	483.61	913.17	940.20
G1-*t*-butyl	Dendrimer	BTT	1240.56	6	0.806	1.357	35	483.61	756.95	862.09
G2-*t*-butyl	Dendrimer	BTT	2964.73	12	0.337	0.568	47	483.61	756.95	862.09
G3-*t*-butyl	Dendrimer	BTT	6413.07	24	0.156	0.262	49	483.61	756.95	862.09
G1-4-heptyl	Dendrimer	BTT	1493.04	6(12)[a]	0.670	0.983(1.966)[a]	-2	483.61	1009.42	988.32
G2-4-heptyl	Dendrimer	BTT	3469.70	12(24)[a]	0.423	0.423(0.846)[a]	—	483.61	1009.42	988.32

[a] Figures in brackets are derived from consideration of the 4-heptyl surface group as 2 chain ends.

ends) and a new approach that relates T_g to mathematical constants that define the geometric relationship of molecular weight increase and generation number, thereby essentially reducing the end group number to a mass relationship.

Conventional Flory–Fox analysis of T_g

The Flory–Fox equation is shown in eqn (1) and a plot of T_g *vs.* $1/M$ generates a straight line with a slope K (a polymer-dependent constant) and a predicted $T_{g\infty}$, determined by the intercept at the y axis.

$$T_g = T_{g\infty} - \frac{K}{M} \quad (1)$$

The conventional Flory–Fox analysis for the ten dendrons synthesised during this study, Fig. 5A, is shown in Fig. 6. Similar plots were generated for the dendrimers with TAEA and BTT cores (ESI†) and the derived $T_{g\infty}$ values are shown in Table 2; correlation coefficients ranged from 0.980 to 0.998. The data suggests that the cyclohexyl functional dendrons are closely approaching the predicted $T_{g\infty}$ at generation 4.

The dendrons with the other functional groups are approximately 10 °C lower than the predicted $T_{g\infty}$ at generation 3; dendrimers with either the TAEA or BTT cores appear to be within 5 °C of their respective $T_{g\infty}$ values by generation 3.

Modified Flory–Fox analysis of T_g

In a relatively early paper investigating the T_g of dendritic polymers, Wooley *et al.*[9] suggested that a modification of the Flory–Fox equation was required and derived eqn (2), where ρ is density, N is Avogadro's number, θ is the free volume per chain end, α is the free volume expansion coefficient, n_e is the number of end groups and M is the molecular weight of the dendritic polymer.

$$T_g = T_{g\infty} - \left(\frac{\rho N \theta}{\alpha}\right)\left(\frac{n_e}{M}\right) \quad (2)$$

As the system specific terms (ρ, N, θ and α) are constant, a simplified equation, eqn (3) was derived which closely resembles the Flory–Fox equation, eqn (1). This was however modified further to incorporate a corrective second term, eqn (4), due to

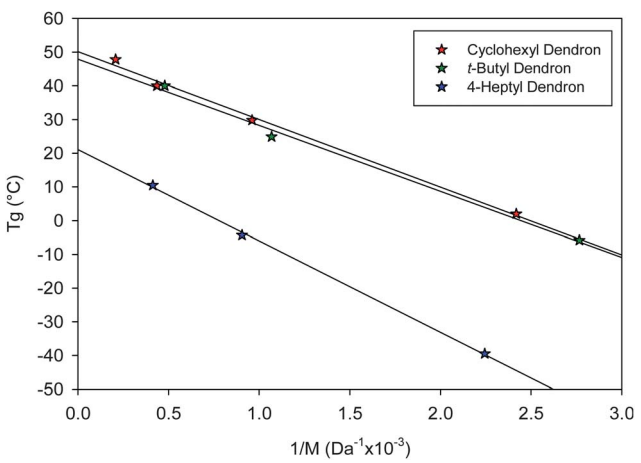

Fig. 6 Flory–Fox analysis of T_g *vs.* 1/M for polyurethane dendrons.

Table 2 Determined values of $T_{g\infty}$ for all study materials

Surface Functionality	Type	Core	$T_{g\infty}$ (°C)[a]
cyclohexyl	Dendron	—	50.114
t-butyl	Dendron	—	48.875
4-heptyl	Dendron	—	21.071
cyclohexyl	Dendrimer	TAEA	47.795
t-butyl	Dendrimer	TAEA	52.301
4-heptyl	Dendrimer	TAEA	23.450
cyclohexyl	Dendrimer	BTT	52.457
t-Butyl	Dendrimer	BTT	53.029
4-heptyl	Dendrimer	BTT	—

[a] $T_{g\infty}$ values are shown to 3 decimal places to emphasise similarity of techniques.

the finite, and constant, value of n_e/M at infinite molecular weight in dendritic polymers, Fig. 7.

$$T_g = T_{g\infty} - K'\left(\frac{n_e}{M}\right) \quad (3)$$

$$T_g = T_{g\infty} - K'\left(\frac{n_e}{M} - \left(\frac{n_e}{M}\right)_\infty\right) \quad (4)$$

As for the Flory–Fox equation, a plot of experimental T_g *vs.* $[n_e/M - (n_e/M)_\infty]$ will produce a prediction of $T_{g\infty}$ at the *y*-axis intercept of the straight line however to exploit this approach, the values for $(n_e/M)_\infty$ must be derived mathematically from a plot of n_e/M *vs.* dendrimer generation for each material/surface type of interest, Fig. 7.

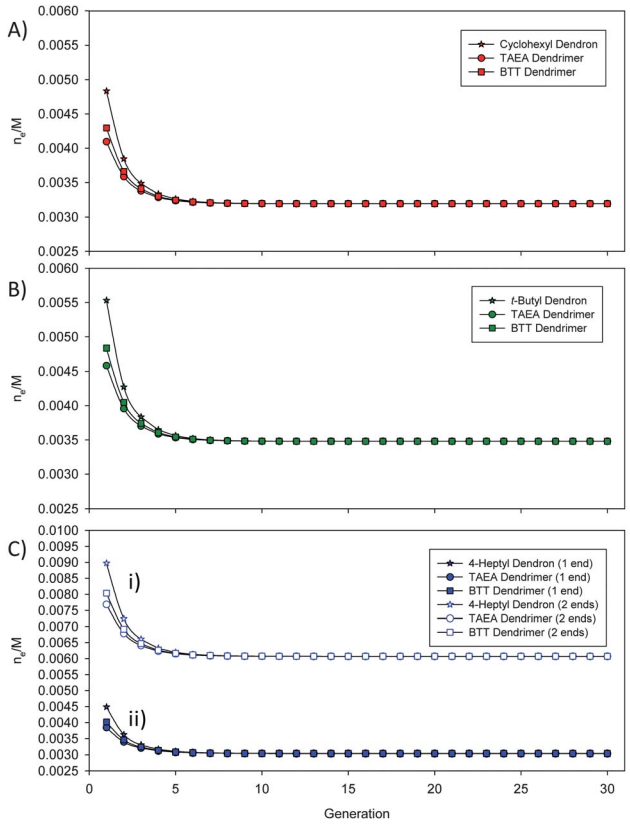

Fig. 7 Determination of $(n_e/M)_\infty$ for polyurethane dendrons and dendrimers with (A) cyclohexyl surface functionality, (B) *t*-butyl surface functionality and (C) heptyl surface functionality considered as either (i) a single chain end or (ii) as two chain ends.

The relationship of n_e/M with dendrimer generation is readily calculated (ESI) as dendritic polymer molecular weight follows a specific geometric progression dependent on the nature and multiplicity of branching and the molecular weight of the constituent repeating and core units. For example, the molecular weight, M, of the cyclohexyl functional dendrons follows a simple progression with respect to generation, G, defined by $M_{Gn} = 2(M_{Gn-1}) + A$ and, due to the AB_2 nature of the branching group, n_e increases as 2^{Gn}. The value A is a constant correction factor which relates to the core chemistry (also considering the focal repeat unit of a dendron as a core), and molecular weight but is consistent within each material series, Table 1. For example, all dendrons, irrespective of surface functionality have $A = 213.24$ Da; values of 415.49 Da and 483.61 Da were determined for the TAEA and BTT core dendrimers respectively.

Extrapolation of molecular weight and number of surface groups to very high generation, using this approach, shows a constant value of (n_e/M) after generation 16–18, and $(n_e/M)_\infty$ is determined as 3.1908×10^{-3} Da^{-1} for the cyclohexyl functional materials (ESI). This value of $(n_e/M)_\infty$ is consistent across the dendrons, TAEA and BTT core dendrimers with the cyclohexyl functionality and therefore relates predominantly to the dendron composition. The value changes with respect to the different surface functionalities and $(n_e/M)_\infty$ values of 3.4799×10^{-3} Da^{-1} and 3.0354×10^{-3} Da^{-1} (ESI†) were determined for the materials with the *t*-butyl and 4-heptyl surface functionalities, Fig. 7.

When using this approach, a specific issue arises for functionalities such as the 4-heptyl surface group. When considering the group as a single chain end, the $(n_e/M)_\infty$ value is readily determined however it is also plausible to consider this functionality as possessing two alkyl end groups per 4-heptyl chain and therefore n_e increases as 2^{G+1} and a value of 6.0708×10^{-3} Da^{-1} is determined for $(n_e/M)_\infty$, Fig. 7Ci. This value is exactly double the value determined by considering the 4-heptyl group as a single chain end and is potentially important in the determination of $T_{g\infty}$ using eqn (4).

The plots of T_g *vs.* $[n_e/M - (n_e/M)_\infty]$ for each series of materials were constructed as described for the conventional Flory–Fox approach and $T_{g\infty}$ values were determined. Surprisingly, and contradictory to many earlier reports, the values of $T_{g\infty}$ were identical (to at least three decimal places) to those determined *via* the conventional Flory–Fox equation and shown in Table 1. Also, the treatment of the 4-heptyl group as a single or double end group made no difference to the calculated $T_{g\infty}$ but simply modified the slope of the straight line plot. The analysis for the ten dendrons is shown in Fig. 8, with additional plots for the 4-heptyl functional dendron plotted as (a) considering the 4-heptyl group as 2 chain ends, and (b) using the conventional Flory–Fox analysis.

As can be readily observed, the three plots for the 4-heptyl functional materials converge on exactly the same value for $T_{g\infty}$ and this is seen for all materials, dendron or dendrimer, within this study (ESI†). No negative influence of the focal point functionality was seen, as reported by, and corrected for, in previous studies.

It is surprising that the original Wooley *et al.*[9] report introducing eqn (2)–(4), did not demonstrate and compare the conventional Flory–Fox analysis of the twenty-two dendritic materials studied, however we have reanalysed the data within the early report and find that both approaches determine an identical value of $T_{g\infty}$ (ESI†) with the plots differing only in slope.

Analysis of T_g using geometric parameters

The strong correlation we have observed between the conventional Flory–Fox analysis and the end group-modified Flory–Fox analysis suggests a relationship between both approaches that has been overlooked in the assumptions that both the number of end groups and the non-zero value of $(n_e/M)_\infty$ play important roles in $T_{g\infty}$ determination for dendritic polymers. We have therefore derived a new approach that examines the modified Flory–Fox equation solely using the factors derived from the geometric progression of dendritic polymer molecular weight and defines end group number purely in terms of factors relating to molecular weight.

As stated earlier, the geometric progression of dendrimer molecular weight can be represented as eqn (5), where A is a correction factor that relates to the molecular weights of its components and is readily calculated (ESI†).

$$M_{Gn} = 2(M_{Gn-1}) + A \tag{5}$$

Considering the case of the generation 1 dendritic polymer, another constant of the geometric progression, B, can be determined as described in eqn (6), and is purely the molecular weight of the generation 1 polymer minus the correction factor. Values of B for the polyurethane materials within our study are included in Table 1. Unlike the constant A, B varies with both surface functionality and dendrimer core chemistry.

$$B = M_{G1} - A \tag{6}$$

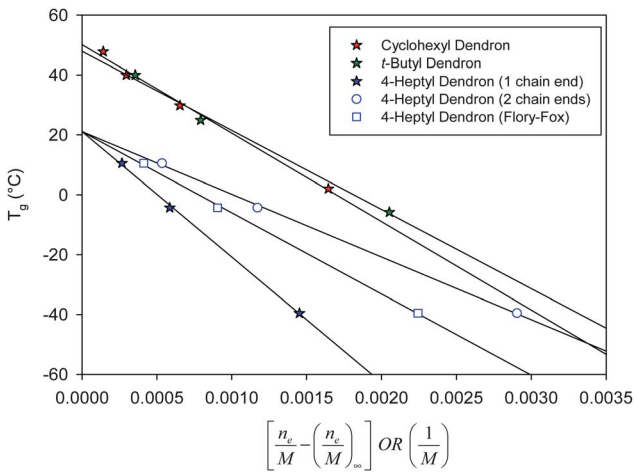

Fig. 8 Comparison of $T_{g\infty}$ using conventional and modified Flory–Fox analysis.

Scaling of dendritic polymer molecular weight based on AB_2 branching can be described purely in terms of the constants A and B, eqn (7), and further simplified to yield eqn (8).

$$M_{Gn} = B2^{Gn-1} + (A[(2x2^{Gn-1}) - 1]) \tag{7}$$

$$M_{Gn} = B2^{Gn-1} + A2^{Gn} - A \tag{8}$$

The number of end groups, n_e, also scales as a geometric progression which is determined by the multiplicity of the core, D, branching group (in this case 2) and generation, eqn (9).

$$n_{e,Gn} = D2^{Gn} \tag{9}$$

The term n_e/M can now be described purely in terms of generation, core multiplicity and the geometric constants A and B for any given dendritic polymer series, eqn (10), and simplified to give eqn (11).

$$\frac{n_{e,Gn}}{M_{Gn}} = \frac{D2^{Gn}}{B2^{Gn-1} + A2^{Gn} - A} \tag{10}$$

$$\frac{n_{e,Gn}}{M_{Gn}} = \frac{D}{\frac{B}{2} + A - \frac{A}{2^{Gn}}} \tag{11}$$

A new constant, C, may be defined as $B/2 + A$ to aid further simplification and the derivation of eqn (12). Values of C are shown in Table 1 and show a lack of dependence on dendrimer core type.

$$\frac{n_{e,Gn}}{M_{Gn}} = \frac{D}{C - \frac{A}{2^{Gn}}} \tag{12}$$

As a dendritic polymer approaches infinite molecular weight, the term $A/2^{Gn}$ approaches zero therefore the term $(n_e/M)_\infty$ approaches a constant value calculated as D/C. It is now readily seen that the term $[n_e/M - (n_e/M)_\infty]$ can be represented purely in terms of A, C and D, eqn (13), which yields eqn (14) and subsequently eqn (16) *via* eqn (15).

$$\frac{n_{e,Gn}}{M_{Gn}} - \left(\frac{n_e}{M}\right)_\infty = \frac{D}{C - \frac{A}{2^{Gn}}} - \frac{D}{C} \tag{13}$$

$$\frac{n_{e,Gn}}{M_{Gn}} - \left(\frac{n_e}{M}\right)_\infty = \frac{CD - D\left(C - \frac{A}{2^{Gn}}\right)}{C\left(C - \frac{A}{2^{Gn}}\right)} \tag{14}$$

$$\frac{n_{e,Gn}}{M_{Gn}} - \left(\frac{n_e}{M}\right)_\infty = \frac{D\frac{A}{2^{Gn}}}{C^2 - C\frac{A}{2^{Gn}}} \tag{15}$$

$$\frac{n_{e,Gn}}{M_{Gn}} - \left(\frac{n_e}{M}\right)_\infty = \frac{DA}{2^{Gn}C^2 - CA} \tag{16}$$

Eqn (16) may be incorporated into eqn (4) to yield eqn (17). As the term D and A are constants, derived from the specific

dendritic polymer, these terms may be incorporated into the constant K′, yielding a new constant K″ and the simplified eqn (18). This suggests that a plot of $T_{g,Gn}$ *vs.* $1/(2^{Gn}C^2 - CA)$ will generate a straight line with a slope K″ and a *y*-axis intercept of $T_{g\infty}$.

$$T_{g,Gn} = T_{g\infty} - K'\left(\frac{DA}{2^{Gn}C^2 - CA}\right) \quad (17)$$

$$T_{g,Gn} = T_{g\infty} - K''\left(\frac{1}{2^{Gn}C^2 - CA}\right) \quad (18)$$

The implications of eqn (18) are that $T_{g\infty}$ may be determined purely using the constants *C* and *A*, and the dendritic polymer generation, *G*. Both *C* and *A* are mass terms and plots derived from eqn (18) do not require consideration of whether the material is a dendrimer or dendron, core multiplicity, end group type or number of end groups. Eqn (18) is therefore a modification of the Flory–Fox equation only in defining the mass term *M* through geometric parameters of the evolution of molecular weight with generation. The assumptions that the unusual number of end groups, lack of entanglement or globular nature of dendritic polymers require specific inclusion within any analysis of T_g appear to be unfounded.

The term $1/(2^{Gn}C^2 - CA)$ has units of Da^{-2} and is therefore highly related to the Flory–Fox equation and the modified Flory–Fox equation (eqn (4)). As such, it is expected that the value of $T_{g\infty}$ derived from all three analyses will be identical but the plots will exhibit different slopes as the constants K, K′ and K″ contain different terms.

Eqn (18) was utilised to generate the analogous T_g *vs.* $1/(2^{Gn}C^2 - CA)$ plots for all of the polyurethane materials generated during this study. Two examples of the analyses, cyclohexyl functional dendrimers (BTT core) and 4-heptyl functional dendrimers (TAEA core) are shown in Fig. 9 and a comparison of the Flory–Fox and modified Flory–Fox analyses is included for one of the examples.

As can be seen, although the slopes are different, the three analyses lead to identical values (at least three decimal places) for $T_{g\infty}$ (ESI†). When applied to the polyurethane materials described here, all analyses gave $T_{g\infty}$ values as shown in Table 2.

Finally, re-analysis of the original data within the Wooley *et al.*[9] report using the geometric progression approach described above (eqn (18); A = 104 Da, B = 216 Da, C = 212 Da) generated identical results to the Flory–Fox and modified Flory–Fox equation within 2 decimal figures (ESI†).

Relationship of T_g with molecular weight

The relationship of T_g *vs.* log*M* is often plotted for linear and dendritic polymers and has been shown to plateau at relatively low generations (generation 3 onwards).[15] The plateau region is rationalised within linear polymer samples as the onset of significant entanglement and therefore the attainment of a consistent T_g. Within dendritic polymers, the expanded-to-globular transition is considered as the most appropriate rationale for the plateau region.

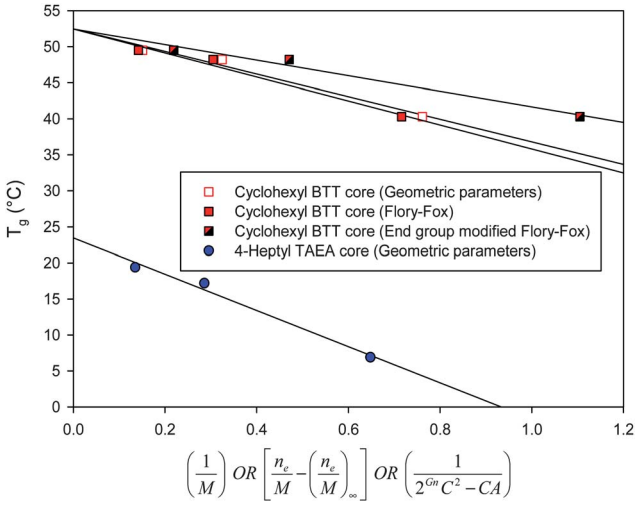

Fig. 9 Comparison of $T_{g\infty}$ determination using geometric parameters, conventional and modified Flory–Fox analyses.

We have plotted all twenty six polyurethane study materials on a single T_g *vs.* log*M* graph, Fig. 10. Interestingly, the dendrimers and dendrons within a surface functionality series, and irrespective of core chemistry, appear to follow a single trend. Additionally, the cyclohexyl functional and the *t*-butyl functional dendritic materials follow a very similar trend within the molecular weight range studied here. This is consistent with the trends for derived $T_{g\infty}$ values shown in Table 2. The 4-heptyl functional materials showed considerably different observed T_g values at all molecular weights and across all material types, again consistent with the results in Table 2.

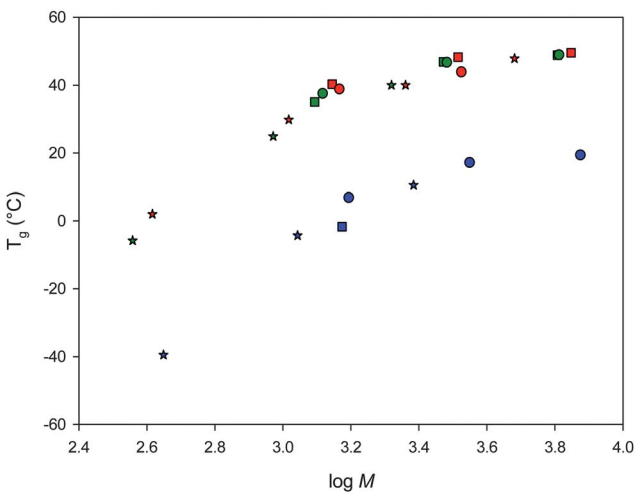

Fig. 10 Variation of T_g with *log M* for all polyurethane dendrons and denrimers synthesised during the study (stars = dendrons, circles = TAEA core dendrimers, squares = BTT core dendrimers; red = cyclohexyl, green = *t*-butyl, blue = 4-heptyl surface functionalities).

Conclusions

The selective chemistry of CDI and CDI derivatives has been shown to be effective in the controlled convergent synthesis of a range of new polyurethane dendrons, to generation 4, and dendrimers, to generation 3. Variation of surface functionality and core chemistry has been successfully achieved and highly pure materials have been isolated. The library of twenty-six new materials provided an opportunity to study the effects of dendrimer structure on T_g and during our evaluation, we have seen that the conventional Flory–Fox equation accurately determines $T_{g\infty}$ without the widely accepted modifications for 'dendrimer-relevant' considerations such as the large number of end groups. It appears that early reports claiming the need for the modified approach did not fully compare the T_g *vs.* $1/M$ relationship for the aromatic ether dendrimer materials studied. Our re-analysis of the early data has shown no significant difference to the conventional Flory–Fox analysis.

During the evaluation, it became clear that the factors M and n_e may be represented purely in terms of the generation dependent geometric progression of molecular weight. A new approach to dendrimer $T_{g\infty}$ determination has therefore been developed which generates identical values to the Flory–Fox equation and is independent of dendrimer chemistry, core/end group multiplicity or bias from the analysis of dendrons or dendrimers. Indeed, the derivation of this approach directly from the previously reported modified Flory–Fox equation, and the reduction of this modified equation solely to mass-related terms, demonstrates the actual relationship of all approaches studied here to dendrimer molecular weight. Each approach simply provides a different multiplier that modifies the slope of the T_g *vs.* molecular weight relationship but has no influence on the intercept and resulting determination of $T_{g\infty}$.

Within the study of T_g, the effect of surface functionality changes were most evident for the flexible 4-heptyl surface group, showing significantly lower T_g than comparable materials with different surface groups. The presence of cyclohexyl and *t*-butyl groups yielded very similar values of T_g across all dendrons and dendrimers studied, that lie on a similar T_g *vs.* log M curve.

Future studies will aim to establish the validity of the use of geometric parameters in the evaluation of $T_{g\infty}$ across a wide range of dendrimer chemistries and investigate the need for variation from the conventional Flory–Fox approach to $T_{g\infty}$ determination.

Acknowledgements

The authors wish to thank the Engineering and Physical Sciences Research Council (EPSRC) and Unilever for funding. Rob Rannard is also warmly thanked for help compiling the manuscript. Considerable thanks are also extended to Prof. Norman Billingham (University of Sussex) for proof-reading and discussion regarding the implications of the geometric progression approach presented.

References

1 (*a*) B. I. Voit and A. Lederer, *Chem. Rev.*, 2009, **109**, 5924; (*b*) C. C. Lee, J. A. MacKay, J. M. J. Fréchet and F. C. Szoka, *Nat. Biotechnol.*, 2005, **23**, 1517.
2 M. Calderón, M. A. Quadir, M. Strumia and R. Haag, *Biochimie*, 2010, **92**, 1242.
3 J. M. J. Fréchet, *J. Polym. Sci., Part A: Polym. Chem.*, 2003, **41**, 3713.
4 (*a*) M. Malkoch, E. Malmström and A. Hult, *Macromolecules*, 2002, **35**, 8307; (*b*) S. P. Rannard and N. J. Davis, *J. Am. Chem. Soc.*, 2000, **122**, 11729; (*c*) M. S. Diallo, L. Balogh, A. Shafagati, J. H. Johnson, W. A. Goddard and D. A. Tomalia, *Environ. Sci. Technol.*, 1999, **33**, 820; (*d*) S. Rannard, N. Davis and H. McFarland, *Polym. Int.*, 2000, **49**, 1002; (*e*) F. Aulenta, M. G. B. Drew, A. Foster, W. Hayes, S. Rannard, D. W. Thornthwaite, D. R. Worrall and T. G. A. Youngs, *J. Org. Chem.*, 2005, **70**, 63; (*f*) T. M. Hermans, M. A. C. Broeren, N. Gomopoulos, P. van der Schoot, M. H. P. van Genderen, N. A. J. M. Sommerdijk, G. Fytas and E. W. Meijer, *Nat. Nanotechnol.*, 2009, **4**, 721; (*g*) T. Darbre and J.-L. Reymond, *Curr. Top. Med. Chem.*, 2008, **8**, 1286; (*h*) S. Grayson and J. M. J. Fréchet, *Org. Lett.*, 2002, **4**, 3171; (*i*) P. Ortega, M. J. Serramia, M. A. Munoz-Fernandez, F. Javier de la Mata and R. Gomez, *Tetrahedron*, 2010, **66**, 3326; (*j*) C. L. Feng, M. Yin, D. Zhang, S. Zhu, A. M. Caminade, J. P. Majoral and K. Muellen, *Macromol. Rapid Commun.*, 2011, **32**, 679; (*k*) L.-L. Lai, H.-C. Hsu, S.-J. Hsu and K.-L. Cheng, *Synthesis*, 2010, 3576; (*l*) S. M. Waybright, K. McAlpine, M. Laskoski, M. D. Smith and U. H. F. Bunz, *J. Am. Chem. Soc.*, 2002, **124**, 8661.
5 (*a*) D. Astruc, E. Boisselier and C. Ornelas, *Chem. Rev.*, 2010, **110**, 1857; (*b*) T. Garg, O. Singh, S. Arora and R. S. R. Murthy, *Int. J. Pharma. Sci. Rev. Res.*, 2011, **7**, 211; (*c*) R. Saraswathi and S.-M. Chen, "*Nanostructured Materials for Electrochemical Biosensors*", Nova Publishers, Ed. Y. Umasankar, S. A. Kumar and S.-M. Chen, 2009, 1, 1; (*d*) O. Flomenbom, J. Klafter, R. J. Amir and D. Shabat, "*Energy Harvesting Materials*" Ed. D. L. Andrews, 2005, 245; (*e*) C. C. Cyran, Y. Fu, H.-J. Raatschen, V. Rogut, B. Chaopathomkul, D. M. Shames, M. F. Wendland, B. M. Yeh and R. C. Brasch, *J. Magn. Reson. Imaging*, 2008, **27**, 581; (*f*) N. Nishiyama, W.-D. Jang and K. Kataoka, *New J. Chem.*, 2007, **31**, 1074; (*g*) E. Murugan and G. Vimala, *J. Colloid Interface Sci.*, 2011, **357**, 354.
6 (*a*) W. J. Feast, S. P. Rannard and A. Stoddart, *Macromolecules*, 2003, **36**, 9704; (*b*) R. T. Taylor and U. Puapaiboon, *Tetrahedron Lett.*, 1998, **39**, 8005; (*c*) B. Bruchmann, *Macromol. Mater. Eng.*, 2007, **292**, 981; (*d*) S. P. Rannard, N. J. Davis and I. Herbert, *Macromolecules*, 2004, **37**, 9418.
7 K. Karatasos, *Macromolecules*, 2006, **39**, 4619.
8 (*a*) A.-M. Caminade, R. Laurent and J.-P. Majoral, *Adv. Drug Delivery Rev.*, 2005, **57**, 2130; (*b*) T. Tuuttila, M. Lahtinen, N. Kuuloja, J. Huuskonen and K. Rissanen, *Thermochim. Acta*, 2010, **497**, 101; (*c*) T. Tuuttila, M. Lahtinen, J. Huuskonen and K. Rissanen, *Thermochim. Acta*, 2010, **497**, 109.
9 K. L. Wooley, C. J. Hawker, J. M. Pochan and J. M. J. Fréchet, *Macromolecules*, 1993, **26**, 1514.
10 T. G. Fox and P. J. Flory, *J. Appl. Phys.*, 1950, **21**, 581.
11 (*a*) B. M. Tande, N. J. Wagner and Y. H. Kim, *Macromolecules*, 2003, **36**, 4619; (*b*) F. Moingeon, P. Masson and S. Méry, *Macromolecules*, 2007, **40**, 55.
12 A. W. Bosman, M. J. Bruining, H. Kooijman, A. L. Spek, R. A. J. Janssen and E. W. Meijer, *J. Am. Chem. Soc.*, 1998, **120**, 8547.
13 (*a*) H. Ihre, A. Hult, J. M. J. Fréchet and I. Gitsov, *Macromolecules*, 1998, **31**, 4061; (*b*) C.-O. Turrin, V. Maraval, J. Leclaire, E. Dantras, C. Lacabanne, A.-M. Caminade and J.-P. Majoral, *Tetrahedron*, 2003, **59**, 3965; (*c*) J. Ropponen, J. Tamminen, M. Lahtinen, J. Linnanto, K. Rissanen and E. Kolehmainen, *Eur. J. Org. Chem.*, 2005, 73; (*d*) J. Ropponen, T. Tuuttila, M. Lahtinen, S. Nummelin and K. Rissanen, *J. Polym. Sci., Part A: Polym. Chem.*, 2004, **42**, 5574; (*e*) O. Ozturk, T. J. Black, K. Perrine, K. Pizzolato, C. T. Williams, F. W. Parsons, J. S. Ratliff, J. Gao, C. J. Murphy, H. Xie, H. J. Ploehn and D. A. Chen, *Langmuir*, 2005, **21**, 3998.
14 P. J. Farrington, C. J. Hawker, J. M. J. Fréchet and M. E. Mackay, *Macromolecules*, 1998, **31**, 5043.
15 K.-I. Akabori, H. Atarashi, M. Ozawa, T. Kondo, T. Nagamura and K. Tanaka, *Polymer*, 2009, **50**, 4868.

